Available online at www.sciencedirect.com
SCIENCE DIRECT®
International Journal of Heat and Mass Transfer 49 (2006) 3800–3806
International Journal of HEAT and MASS TRANSFER
www.elsevier.com/locate/ijhmt

Further study on the influence of particle coating on fluidized bed heat transfer

Jerry Sjösten [a,1], Mohammad R. Golriz [a], John R. Grace [b,*]

[a] Department of Applied Physics and Electronics, Umeå University, SE-90187 Umeå, Sweden
[b] Department of Chemical and Biological Engineering, University of British Columbia, 2360 East Mall, Vancouver, BC, Canada V6T 1Z3

Received 26 October 2005; received in revised form 30 March 2006
Available online 9 June 2006

Abstract

Heat transfer to an immersed sphere from fluidized uncoated sand particles of different mean size and size distribution is compared with that from coated sand particles of equal size extracted from two full-scale fluidized bed boilers for different superficial gas velocities and mean particle diameters from 350 to 646 μm. The thin coating on the sand bed particles from full-scale boilers was found to have a significant effect on the heat transfer coefficient, while the particle size distributions, as well as coating thickness, had little or no influence on the heat transfer coefficients for the conditions investigated.

Keywords: Fluidized bed; Heat transfer; Particle coating; Combustion; Biomass

1. Introduction

Fluidized bed boilers are now widespread for power generation and raising steam by combustion of coal, biomass, petroleum coke, etc. Surface-to-bed heat transfer in fluidized beds depends on a number of parameters, including such particle properties as the mean particle diameter, size distribution, sphericity, specific heat, and thermal conductivity. In a number of fluidized bed processes, particle properties change with time as a result of coating on their surfaces. For example, during biomass combustion ash-forming elements may form coatings on the bed material particles (usually sand), and as their melting temperatures are approached, particles agglomerate. The heat transfer coefficient may then change as the particle surfaces are coated, possibly leading to decreased heat transfer [1]. While considerable work has been done on fluidized bed heat transfer in general (e.g., see [2–5]) there are few investigations on the influence of particle coatings on the heat transfer coefficient.

Sjösten et al. [1] carried out preliminary heat transfer measurements for two stainless steel spheres of diameter 10 and 15 mm and an aluminum alloy cylinder of 4-mm diameter and 40 mm length mounted vertically in a cold laboratory-scale bubbling fluidized bed. All three indicated that a higher heat transfer coefficient is achieved with uncoated particles than with coated particles. In this paper we provide new data and consider the influence of the coating thickness of sand particles on the convective/conductive heat transfer coefficients for exchange with a relatively large sphere immersed in bubbling fluidized beds, as well as the influence of mean particle size and size distribution. We also offer a plausible explanation for the differences in the behavior of the BFB and CFB particle coatings.

2. Experimental apparatus and materials

Experiments were carried out in an electrically grounded cylindrical Plexiglas column of inner diameter 90 mm and height 263 mm. The distributor was a 1-mm thick steel plate with 47 perforations of diameter 1 mm on a 12-mm

* Corresponding author. Tel.: +1 604 822 3121; fax: +1 604 822 6003. *E-mail address:* jgrace@chml.ubc.ca (J.R. Grace).
[1] Present address: Cool Engineering AB, Arödsindustriväg 60, S-422 43 HisingsBacka, Sweden.

0017-9310/$ - see front matter
doi:10.1016/j.ijheatmasstransfer.2006.03.033

Nomenclature

A_S	sphere surface area, m^2	T_{ini}	sphere initial temperature, °C
$C_{p,sphere}$	specific heat of test sphere, J/kg K	T_{sphere}	test sphere temperature, °C
d_p	mean particle diameter, m	U	superficial gas velocity, m/s
h	convective heat transfer coefficient, W/m^2 K	U_{mf}	minimum fluidization velocity, m/s
k_{sphere}	thermal conductivity of test sphere material, W/m K		
m_{sphere}	mass of sphere, kg	*Greek symbols*	
t	elapsed time, s	ε_{mf}	voidage at minimum fluidization, –
T_{bed}	bed temperature, °C	φ	sphericity, –
		ρ_p	particle density, kg/m^3

square pitch giving a total open area ratio of 0.6%. A thermocouple 54 mm above the distributor plate, on the axis of the column, measured the bed temperature. Expanded bed heights were determined visually and from pressure gradients, as described by Werther [6]. Filters at the top of the column prevented particle egress. The fluidizing gas was dry (<10% RH) compressed air at room temperature. For each experiment the static bed height was ∼110 mm.

The convective/conductive heat transfer coefficient was measured using a 15-mm diameter stainless steel A316 sphere, supported on a stainless steel tubular handle of length 400 mm and 4 and 6 mm inner and outer diameters, respectively, as shown in Fig. 1. The sphere was first heated in an oven to ∼145 °C, and then plunged vertically into the fluidized bed from above. Its temperature was then measured as a function of time. A thermocouple was inserted to the bottom of a hole of diameter 1.5-mm drilled to the center of the sphere. To reduce the thermal contact resistance between the thermocouple and sphere, the bottom of the hole was filled with non-silicon heat paste from Wentworth House. To reduce heat losses, the sphere was fastened to the handle with as little contact area as possible, using a 20-mm aluminium oxide tube of 2-mm o.d. (3), and the joint was "cemented" with Plastic Padding Chemical Metal (Loctite Sweden AB). To reduce lateral and axial movement during the measurements, a 50-mm Plexiglas plug was installed on the handle (see Fig. 1).

Pressure differences were determined by a U-type manometer and a pressure transducer (TESTO 452 and 0638.1545; Nordtec Instrument, Sweden). The airflow was measured and controlled by a Brooks mass flow controller (model 5853i, 550 SLPM). Temperatures were measured by T-type thermocouples and recorded by a data acquisition system consisting of a Data Taker (DT100, version 3.5) data-logger and personal computer.

The uncoated sands were obtained a few hours after completely replenishing the sand in two Swedish boilers, a 90-MW_{th} CFB (Foster Wheeler) boiler owned by Skellefteå Kraft, and a 30-MW_{th} BFB (Ahlström) boiler operated by Falun Energi. The coated sands were sampled after the boilers had been operating for 7 and 17 days (CFB) or 7 and 33 days (BFB) after changing the bed material. Table 1 gives the particle size distributions. For each plant, samples were taken at prescribed intervals during a period of roughly 3–5 weeks. Since bed material was exchanged at regular intervals during the sampling period, the samples also contained particles that had been in the CFB and BFB units less than 7, 17 or 33 days. Consequently the particles in each sample varied in coating thickness. Age distributions of the particles appear in Fig. 2. To investigate the effect of coatings, nine silica sand mixtures were used.

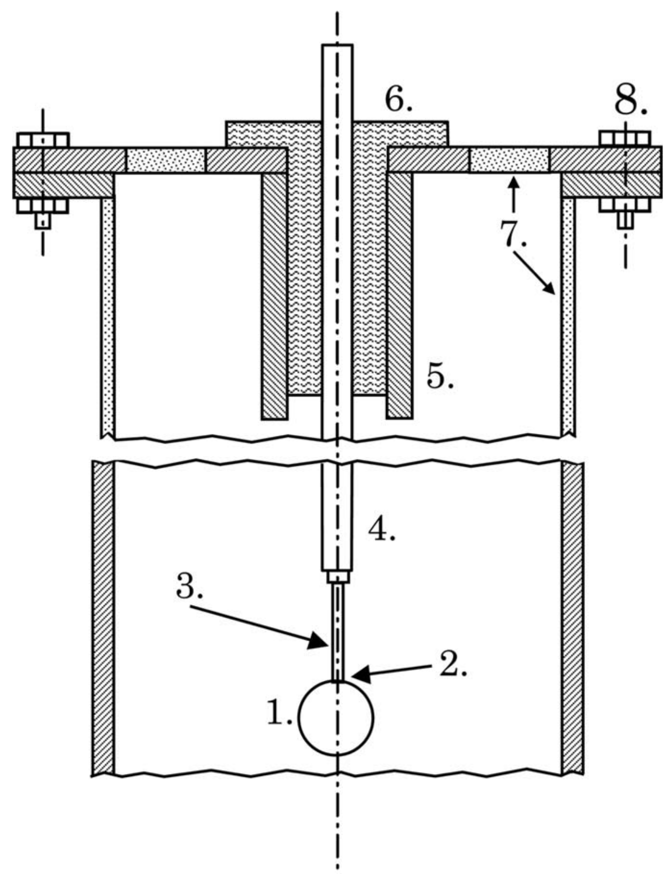

Fig. 1. Schematic of test sphere. (1) 15-mm sphere fastened to handle; (2) junction and sealing of thermocouple; (3) aluminium oxide tube; (4) upper part of handle; (5) supporting cylinder; (6) supporting plug; (7) exhaust air outlet with filter; (8) fastening bolts.

Table 1
Original particle size distributions for CFB and BFB sands

Sieve aperture range, μm	Mass fraction of the sample, %					
	90 MW_{th} CFB boiler			30 MW_{th} BFB boiler		
	Uncoated	Coated, 7 days	Coated, 17 days	Uncoated	Coated, 7 days	Coated, 33 days
8000–16,000	None	1.03[a]	None	None	0.95[a]	1.49[a]
4000–8000	None	0.48[a]	None	None	1.30[a]	3.08[a]
2000–4000	None	0.27	0.25	0.40	2.53	6.29
1000–2000	0.27	0.54	0.82	6.14	19.24	26.41
630–1000	3.54	4.41	6.44	18.76	48.86	46.34
500–630	21.84	15.53	22.76	28.90	21.46	13.67
300–500	54.79	58.03	60.93	43.91	5.51	2.71
250–300	9.12	11.46	6.36	1.41	0.15	None
150–250	9.50	8.25	2.45	0.48	None	None
100–150	0.94	None	None	None	None	None
Mean particle diameter, μm	371	381	420	515	792	937

[a] Agglomerated particles.

Detailed information on these mixtures appears in Table 2. The sand mixtures were of different mean particle diameters and size distributions, see Table 3. The coated particles were sieved to ensure that the coated and uncoated particles had the same mean particle diameter and size distribution in the tests, to isolate the influence of the coating from the increase in mean particle size. The average coating thicknesses of the CFB and BFB particles were approximately 9 and 20 μm, respectively, after 7 days. After 17 days of operation the average coating thickness of the CFB sand particles was 15 μm, whereas after 15 and 33 days the BFB sand had average coating thicknesses of 30 and 47 μm, respectively [1,7]. Typical cross-sections near the surface of bed particles are shown in Fig. 3. Two layers of coating can be identified, inner and outer. The characteristics of these layers are influenced both by the fuel and bed materials. The inner layer seems to be more homogeneous, with a high chemical composition of calcium silicates, whereas the outer heterogeneous layers were more fuel dependent [8]. Chemical compositions were determined by SEM (scanning electron microscopy)/EDS (energy dispersive X-ray spectroscopy) spot analysis, with four spots in the middle of the coating surrounding each particle analyzed. Golriz et al. [8] found that the main elemental compositions were calcium and silicon for both the inner and outer layers. The inner layer contained higher fractions of Si and Ca, and less Mg, P, and Fe, compared with the outer layer, whereas the differences in other elements such as Na, Al, S, K, Ti, Mn, and Zn were negligible.

3. Experimental procedure

Minimum fluidization velocities determined by the procedure recommended by Howard [9], are shown in Table 2. The bed height and pressure gradients were used to determine bed voidages. The (effective) sphericities of the sand particles, estimated using the equation of Ergun [10], also appear in Table 2.

After mixing the bed thoroughly for a few minutes, the heat transfer coefficients were determined for different superficial gas velocities, with the measurements repeated 5–10 times for each setting. All measurements were carried out with the bed at 22 ± 2 °C and atmospheric pressure in the bubbling fluidization flow regime with U/U_{mf} from 1 to 4.

After the test sphere was heated to ~145 °C in the oven, it was cooled in the fluidized bed, with its centre 65 mm above the distributor plate on the axis of the column until its temperature fell to ~10 °C above the bed temperature. The temperature at the sphere centre was recorded at a sampling rate of 1 Hz during the cooling. Since the maximum Biot number for the sphere was 0.08 (Bi < 0.1), the lumped capacitance model was used to calculate the heat transfer coefficient between the probe and the fluidized bed. This assumes that temperature gradients within the sphere are negligible. The time dependence of the sphere temperature is then

$$\ln\left[\frac{T_{\mathrm{sphere}}-T_{\mathrm{bed}}}{T_{\mathrm{ini}}-T_{\mathrm{bed}}}\right] = -\frac{hA_{\mathrm{S}}}{m_{\mathrm{sphere}}C_{p,\mathrm{sphere}}}t \qquad (1)$$

The specific heat and thermal conductivity of the probe were assumed to be independent of temperature and were taken at the average temperature of the sphere during the evaluation period from Touloukian and Buyco [11] and Touloukian et al. [12], respectively. The data subsets used to obtain the heat transfer coefficients by fitting began 5–60 s after immersion of the sphere, and covered periods of duration 25–60 s, with the evaluation period chosen to give coefficients of determination (R^2) as high as possible. For this analysis, R^2 was always >0.99 for the evaluation periods.

Heat transfer coefficients were corrected for heat conduction along the handle, by treating it as a fin of infinite length. This correction was approximately 10%, confirmed with the sphere cooling in air. Uncertainties in determining the heat transfer coefficient and minimum fluidization velocities were estimated at a 95% confidence level by the procedures outlined by Coleman and Steele [13]. The resulting total uncertainty of the determination in h is esti-

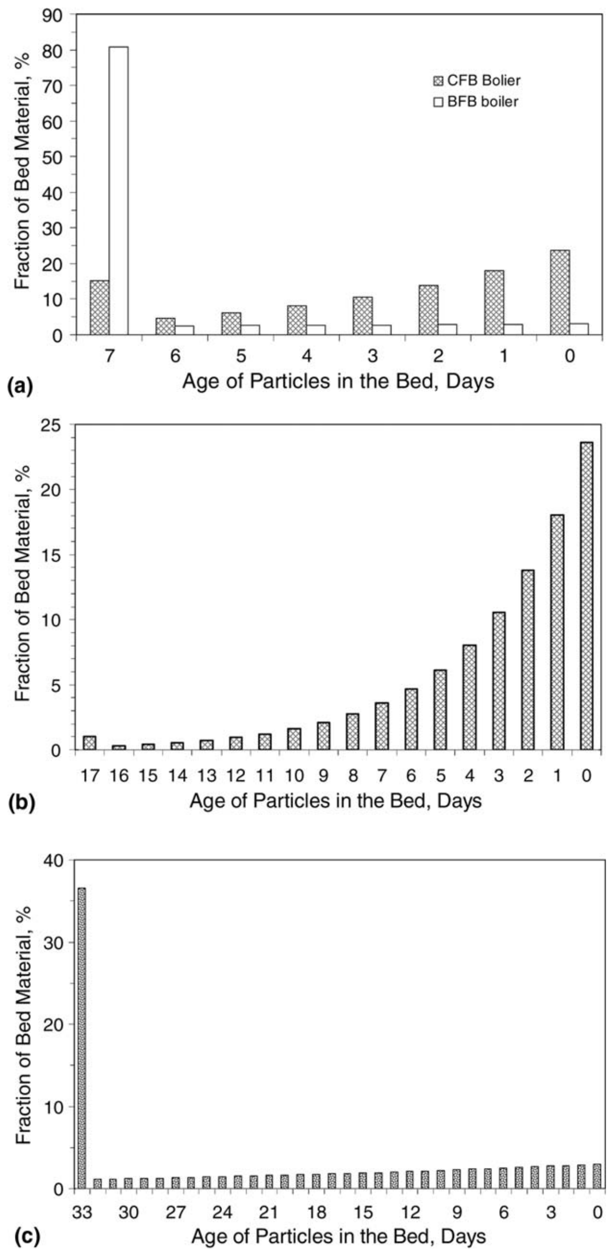

Fig. 2. Estimated age distribution of bed material particles for (a) CFB boiler and BFB boiler after 7 days operation; (b) CFB boiler after 17 days operation; (c) BFB boiler after 33 days operation.

mated to be within ±20% for $U < 1.5U_{mf}$ and within ±12% at higher gas velocities.

4. Results and discussion

The object-to-bed heat transfer coefficient for uncoated and coated CFB particles is seen in Fig. 4 to increase with gas velocity, leveling off at about $2U_{mf}$. The coefficients for the uncoated particles are higher than for the coated particles, especially for $U > 1.5U_{mf}$. The values are almost the same for the 7- and 17-days coating periods, suggesting that the effect of the particle coatings is established at an early stage and that the coating thickness had little influence on the heat transfer. For $U > 1.5U_{mf}$, h was reduced by ∼16% due to the coating.

The heat transfer coefficients for the BFB particles of mean diameter 635 μm appear in Fig. 5. The trends are similar to those for the CFB particles. However, the reduction in h due to coating was lower, ∼8% at higher U/U_{mf}, despite the thicker coating on the BFB sand. Again the heat transfer results were very similar for different coating thicknesses, 20 and 47 μm after 7 and 33 days, respectively. One reason for the stronger effect of coating on the heat transfer coefficient for CFB compared with BFB can be the difference in the chemical composition of the particle coating. Elemental analyses of the particle coatings (in the same CFB, but in a different BFB, with the same fuel as used in our BFB tests) have shown that the BFB coatings contained twice the Si and half the amount of Ca of the CFB particle coatings. The BFB coating had less K and Fe, but more Mg and P, compared with the CFB coating, whereas differences in other elements were negligible [8]. This can be explained by differences in the fuel-mixture, which also contained peat in the CFB case.

Fig. 6 shows the effect of the particle size distribution on the heat transfer coefficients, with the open symbol in each case denoting a narrow distribution and the closed symbol a relatively broad distribution with essentially the same mean particle diameter. The particle size distribution appears to have had little effect on the measured heat transfer coefficient, consistent with Clift and Grace [14] and Geldart [15] who indicated that the particle size distribution

Table 2
Properties of uncoated bed materials in the experiments

Test	1	2	3	4	5	6	7	8	9
Unit	CFB	BFB	BFB	CFB	CFB	CFB	BFB	BFB	BFB
Sampling time, days	0, Uncoated	0, Uncoated	0, Uncoated	7, Coated	7, Coated	17, Coated	7, Coated	7, Coated	33, Coated
d_p range, μm	300–400	560–710	300–1000	300–400	150–710	300–400	560–710	300–1000	560–710
$\bar{d}_p$, μm	350	635	646	350	352	350	635	646	635
ρ_p, kg/m^3	2630	2580	2580	2510	2510	2510	2530	2530	2530
U_{mf}, m/s	0.15	0.35	0.36	0.14	0.14	0.15	0.39	0.40	0.34
ε_{mf}, –	0.47	0.48	0.47	0.49	0.49	0.50	0.48	0.49	0.47
φ, –	0.83	0.73	0.76	0.76	0.76	0.76	0.81	0.77	0.76

Table 3
Size distributions of sand particles in the experiments

Sieve aperture range, μm	Mass fraction of bed material, %			
	Tests 1, 4 and 6	Test 5	Tests 3 and 8	Tests 2, 7 and 9
710–1000	–	None	29.1	–
630–710	–	3.9	30.3	100[b]
560–630	–	8.3	20.6	
500–560	–	8.3	11.6	
400–500	–	50.0[a]	7.7	–
300–400	100	–	0.7	–
250–300	–	17.1	None	–
150–250	–	12.3	None	–
Mean particle diameter, μm	350	352	646	635

[a] Mass fraction of particles with $300 < d_p < 500$.
[b] Mass fraction of particles with $560 < d_p < 710$.

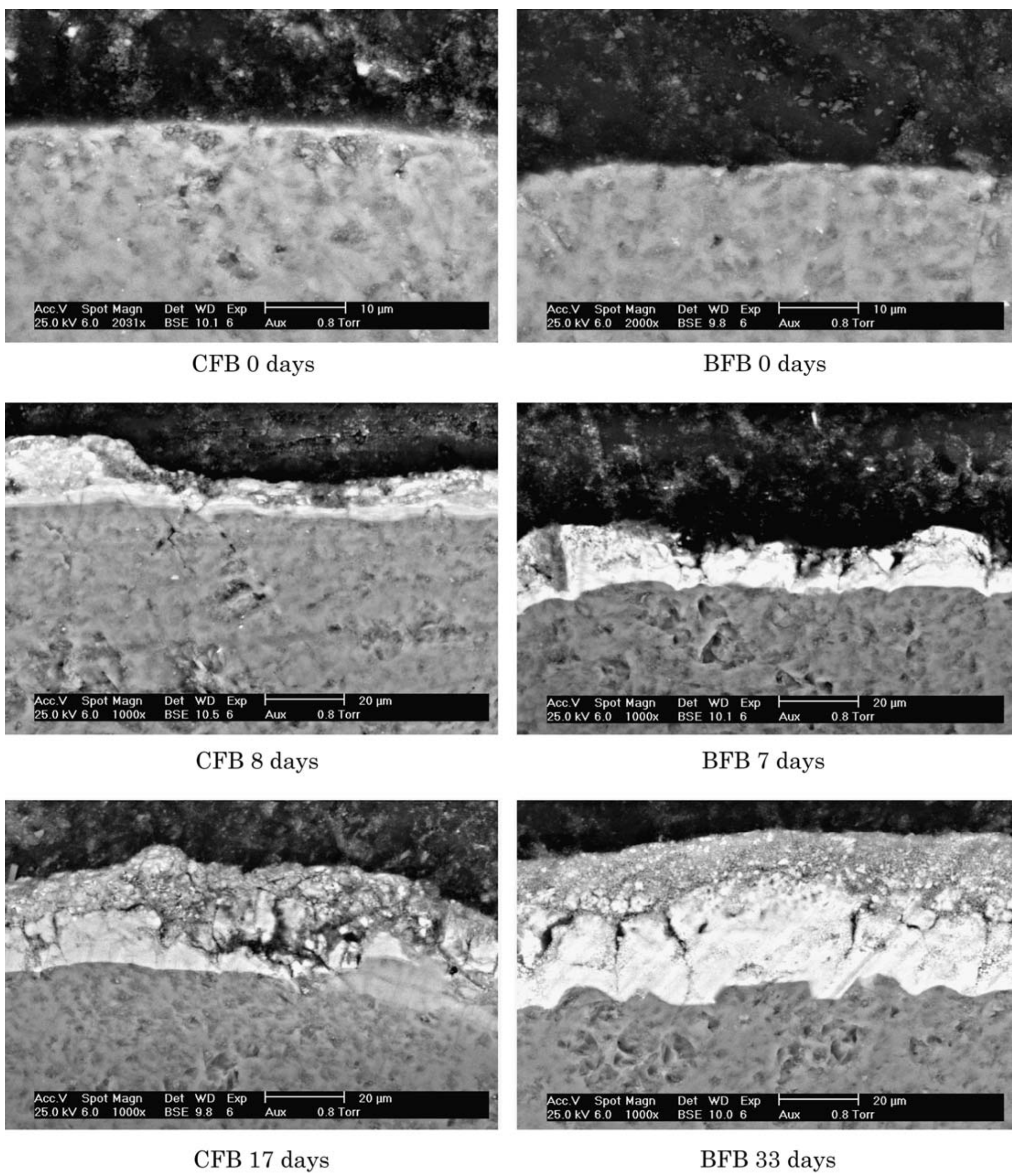

Fig. 3. SEM-images of typical cross-sections near the surfaces of bed particles of CFB and BFB boilers.

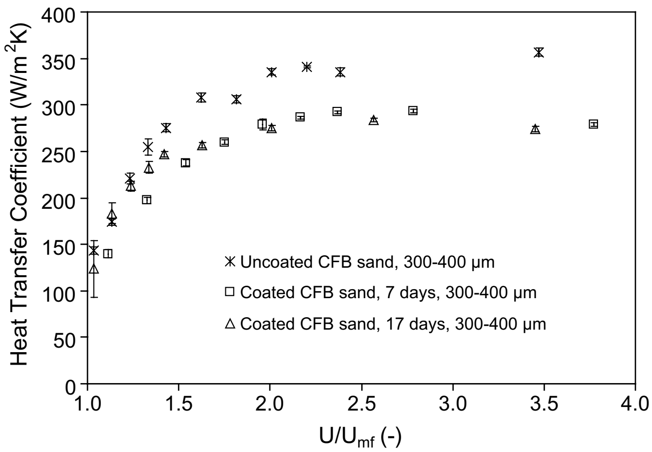

Fig. 4. Mean heat transfer coefficient vs. velocity ratio, U/U_{mf}, for uncoated and coated particles from 90 MW_{th} CFB boiler. For conditions see Table 2. Error bars give 99% confidence intervals.

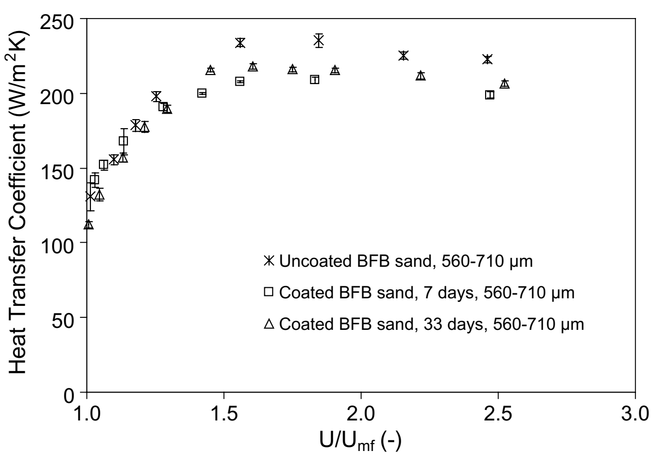

Fig. 5. Mean heat transfer coefficient vs. velocity ratio, U/U_{mf}, for uncoated and coated bed materials from 30 MW_{th} BFB boiler. For conditions see Table 2. Error bars give 99% confidence intervals.

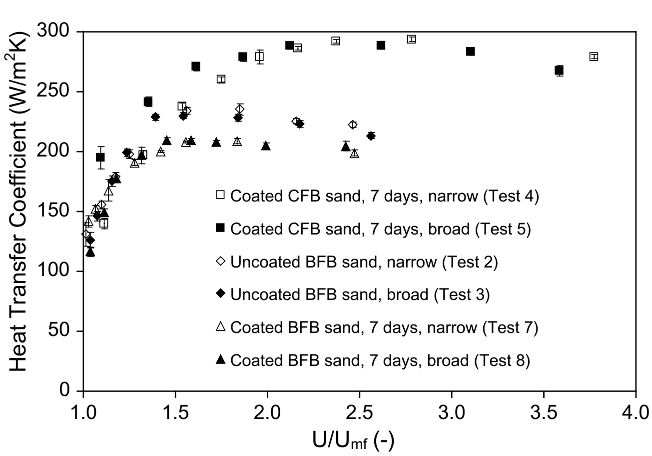

Fig. 6. Influence of particle size distribution on mean heat transfer coefficient for 90 MW_{th} CFB and 30 MW_{th} BFB particles. For conditions see Table 2. For size distributions, see Table 2. Error bars give 99% confidence intervals.

has little effect on the size and frequency of bubbles for group B materials, and therefore on the magnitude of the total convective/conductive heat transfer coefficient [5]. As expected the (maximum) heat transfer coefficient increased with decreasing mean particle diameter.

There is no single unambiguous explanation for the influence of extended residence in fluidized bed combustors on the heat transfer coefficients for the sand particles. Such thin coatings do not appreciably affect bulk particle properties like density and specific heat. The layers could provide some insulating effect, but the particle thermal conductivity is normally of little importance with respect to fluidized bed heat transfer [2,16]. Changes in particle shape as a result of attrition could play some role. However, the most likely explanation is that the surface deposits cause changes in the coefficients of friction and restitution, affecting interactions between particles themselves and between the particles and surfaces (including the heat transfer surface), thereby altering the overall bed hydrodynamics. Experiments by Chang and Louge [17] demonstrated that thin coatings added to glass beads could cause substantial changes in circulating bed hydrodynamics, and bubbling beds may show similar effects.

5. Conclusions

Bed-to-surface convection heat transfer coefficients were measured in a cold fluidized bed loaded with uncoated and coated sand particles of narrow and wide size distributions. Coated particles showed lower heat transfer coefficients than uncoated ones. For $U/U_{mf} > 1.5$ the reductions were 16% and 8% for CFB and BFB sand particles, respectively. However, neither the coating thickness nor the particle size distribution had a significant effect on the measured heat transfer coefficient for the range of conditions investigated.

Acknowledgements

The authors are grateful to Professor A. Nordin and Dr. M. Öhman, Department of Energy Technology and Thermal Process Chemistry, Umeå University, for sharing sand samples.

References

[1] J. Sjösten, M.R. Golriz, A. Nordin, J.R. Grace, Effect of particle coating on fluidized bed heat transfer, Ind. Eng. Chem. Res. 43 (2004) 5763–5769.
[2] J.S.M. Botterill, Fluid-Bed Heat Transfer – Gas-Fluidized Bed Behaviour and its Influence on Bed Thermal Properties, Academic Press, London, 1975 (Chapter 4).
[3] M. Al-Busoul, Prediction of heat transfer coefficient between immersed surfaces and fluidized beds, Int. Comm. Heat Mass Transfer 27 (2000) 549–558.
[4] S.W. Kim, J.Y. Ahn, S.D. Kim, D.H. Lee, Heat transfer and bubble characteristics in a fluidized bed with immersed horizontal tube bundle, Int. J. Heat Mass Transfer 46 (2003) 399–409.
[5] J.C. Chen, J.R. Grace, M.R. Golriz, Heat transfer in fluidized beds: design methods, Powder Technol. 150 (2005) 123–132.

[6] J. Werther, Measurement techniques in fluidized beds, Powder Technol. 102 (1999) 15–36.
[7] E. Brus, M. Öhman, A. Nordin, B.-J. Skrifvars, R. Backman, Bed material consumption in biomass fired fluidized bed boilers due to risk of bed agglomeration – coating formation and possibilities for regeneration, IRFR Combust. J. (2003). Article number 200302.
[8] M.R. Golriz, M. Eriksson, M. Öhman, A. Nordin, R. Backman, Influence of fluidization velocity on bed defluidization in fluidized bed combustors, in: Proceedings of 18th International Fluidized Bed Combustion Conference, Toronto, May 22–25, 2005.
[9] J.R. Howard, Fluidized Bed Technology – Principles and Applications, Adam Hilger, Bristol, 1989 (Chapter 2).
[10] S. Ergun, Fluid flow through packed columns, Chem. Eng. Prog. 48 (1952) 89–94.
[11] Y.S. Touloukian, E.H. Buyco, Specific Heat – Metallic Elements and AlloysThermophysical Properties of Matter, vol. 4, Purdue Research Foundation, Plenum Publishing Corporation, New York, 1970, Data table No. 200, p. 710.
[12] Y.S. Touloukian, R.W. Powell, C.Y. Ho, P.G. Klemens, Thermal Conductivity – Metallic Elements and Alloys, Thermophysical Properties of Matter, vol. 1, Purdue Research Foundation, Plenum, New York, 1970, Data table No. 331, p. 1172.
[13] H.W. Coleman, W.G. Steele Jr., Experimentation and Uncertainty Analysis for Engineers, Wiley, New York, 1989 (Chapter 4).
[14] R. Clift, J.R. Grace, Coalescence of bubble chains in fluidized beds, Trans. Inst. Chem. Eng. 50 (1972) 364–371.
[15] D. Geldart, Types of gas fluidization, Powder Technol. 7 (1973) 285–292.
[16] O. Molerus, K.E. Wirth, Heat Transfer in Fluidized Beds, Chapman & Hall, London, 1997 (Chapter 6).
[17] H. Chang, M. Louge, Fluid dynamic similarity of circulating fluidized beds, Powder Technol. 70 (1992) 259–270.